EVLA Memo #152
Characterizing the Sensitivity of the EVLA at L-band

Emmanuel Momjian and Rick Perley
NRAO

May 2, 2011

Abstract

We present sensitivity measurements of the EVLA at L-band between 0.95 and 2 GHz. These are obtained using three EVLA antennas that are equipped with the final, EVLA-compliant L-band receivers. The reported SEFD values meet and/or exceed the EVLA sensitivity requirements over about 70% of the band, but are too high by 12–38% over the frequency range 1425–1750 MHz.

1 Introduction

A sensitivity analysis of the EVLA at L-band has been performed to measure the performance of the array between 0.95 and 2 GHz, and to assess whether the sensitivity requirements of the EVLA project are met at this frequency band.

2 Observations

EVLA B-configuration observations at various L-band frequencies were carried out on March 8, April 21 and 23, 2011, for a total of 2 hours. The calibrator source 3C286 (J1331+3030) and a field devoid of strong continuum sources (hereafter "blank field") were observed in each session. A total of five frequency settings were utilized in these observations to fully cover the frequency range accessible with the EVLA at L-band. The observing sessions and corresponding frequency settings are listed in Table 1.

For each frequency setting, the WIDAR correlator was configured to deliver a total of 32 sub-bands (16 adjacent sub-bands from each baseband), each with 8 MHz bandwidth and 128 spectral channels, resulting in a spectral resolution of 62.5 kHz. The correlator integration time was 5 seconds.

Date	Frequency Range (MHz)	
	Baseband Pair AC	Baseband Pair BD
March 8, 2011	1190–1318	1300–1428
April 21, 2011	962–1090	1080–1208
April 23, 2011	898–1026	1422–1550
″	1542–1670	1662–1790
″	1782–1910	1902–2030

Table 1: Summary of the Observations

3 Data Reduction and Analysis

Data reduction and analysis were carried out in AIPS. After loading the data, antennas that did not have the EVLA-compliant L-band OMTs were edited out, resulting in a data set with eight antennas. The flux density scale was set using the Baars et al. 1977 coefficients for 3C286. Antenna based delay, complex gain and bandpass calibration solutions were obtained using the data of the calibrator source 3C286 for each sub-band and polarization product (i.e., RR and LL) separately. These solutions were then applied on the visibilities of the blank field, and spectra were generated to visually inspect its data in order to exclude spectral channels and sub-bands that were affected by RFI from subsequent analysis.

Using the AIPS task UVHGM, the RMS noise values for Stokes I were measured by fitting Gaussian profiles on the histogram distributions of the blank field's real part of the visibilities. For this, we used a continuous, RFI-free channel range from each sub-band that was not visibly contaminated by RFI. A 3-channel Hanning-smoothing was applied on the spectra in all the data reduction and analysis steps to reduce the Gibbs ringing phenomenon introduced by strong RFI features at various L-band frequencies.

While the eight antennas included in the data calibration and analysis were equipped with the new, EVLA compliant OMT, only four of these were also equipped with the 4th cryogenic compressor. A forth compressor is being added to all antennas in order to shorten cooling times, reduce the L-band receiver temperature, and improve system sensitivity. With one exception, antennas that were equipped with both the new OMT and the 4th compressor had $\sim$ 15–20% lower system temperatures, as seen in the switched power monitors and in the RMS noise values of the histograms. Therefore, the sensitivity measurements reported in this memo are based on the average values of the baselines among the three EVLA antennas that are fully compliant with the EVLA project requirements. The discrepancy in the sensitivity among the individual baselines of these three antennas was less than 5%.

4 Results

As examples of the Gaussian noise in our data, Figure 1 shows histogram distributions of the blank field data using the visibilities of the baselines among the three, fully EVLA-compliant antennas in four different sub-bands. Also shown are the resulting Gaussian profiles and parameters. The frequency on top of each plot denotes the value at the center of the continuous, RFI-free channel range used in each sub-band.

Multiple background continuum sources in the blank field contribute by a total of $S \sim 50$ mJy to our measurements, as determined by imaging one of the sub-bands. A correction was made to account for these background sources as follows:

$$\mathrm{RMS} = \sqrt{(\mathrm{RMS}_h)^2 - (S)^2}, \tag{1}$$

where RMS_h is the noise values obtained through the histogram fittings.

The corrected RMS noise values were then converted to System Equivalent Flux Densities (SEFDs) using the following equation:

$$\mathrm{RMS~(Jy)} = \frac{1}{2\eta_c \kappa_{hs}} \frac{\mathrm{SEFD~(Jy)}}{\sqrt{\beta\tau}}, \tag{2}$$

where β is the spectral channel width in Hz and τ is the correlator integration time in seconds. η_c is the WIDAR correlator efficiency, and it is assumed to be 0.93 for the mode used in these obser-

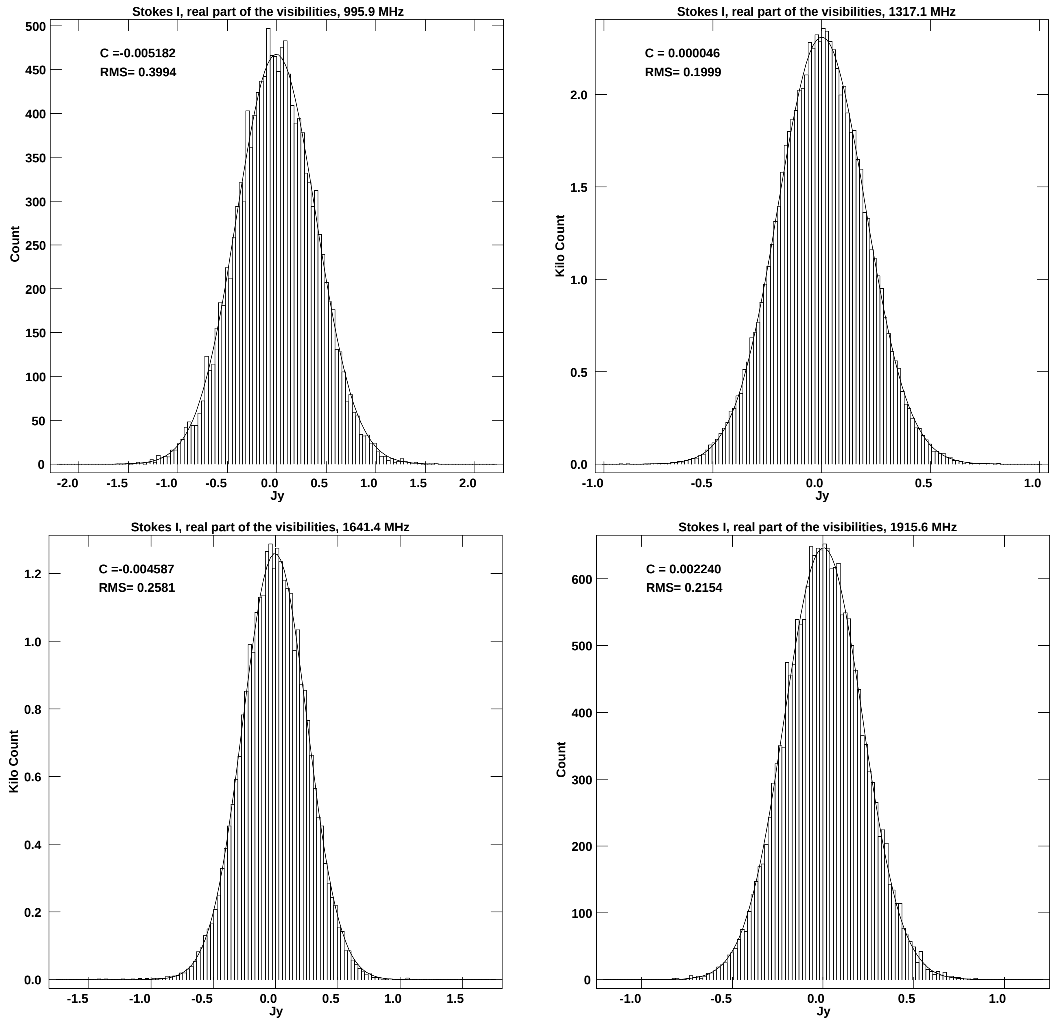

Figure 1: Histogram distributions of the blank field data of the baselines among the three fully EVLA-compliant antennas in four different sub-bands. Also shown are the fitted Gaussian profiles. A continuous, RFI-free channel range per sub-band, Stokes I, and the real part of the visibilities were used to make these histograms and measure the RMS. The correction made to account for the background continuum is not reflected in these histograms nor on the RMS noise values noted in the plots.

vations, and κ_{hs} is the improvement in the signal-to-noise due to the application of the Hanning-smoothing, which is 1.633[1] for a 3-channel Hanning-smoothing.

For the EVLA, we note that the SEFD is related to the system temperature ($T_{\rm sys}$) and the antenna illumination efficiency (A_e) by:

$$\text{SEFD (Jy)} = 5.62\ \frac{T_{\rm sys}\ ({\rm K})}{A_e} \tag{3}$$

Figure 2 shows the SEFD values in the full EVLA L-band frequency range ($\sim 0.95 - 2$ GHz) in black. The EVLA project requirements on the antenna sensitivity in the frequency range 1–2 GHz are overlaid in red. The ‘steps’ at each end are to allow for amplifier and feed edge ‘effects’.

[1]The improvement in signal-to-noise due to a 3-channel Hanning-smoothing is $1/\sqrt{0.25^2 + 0.5^2 + 0.25^2}$=1.633

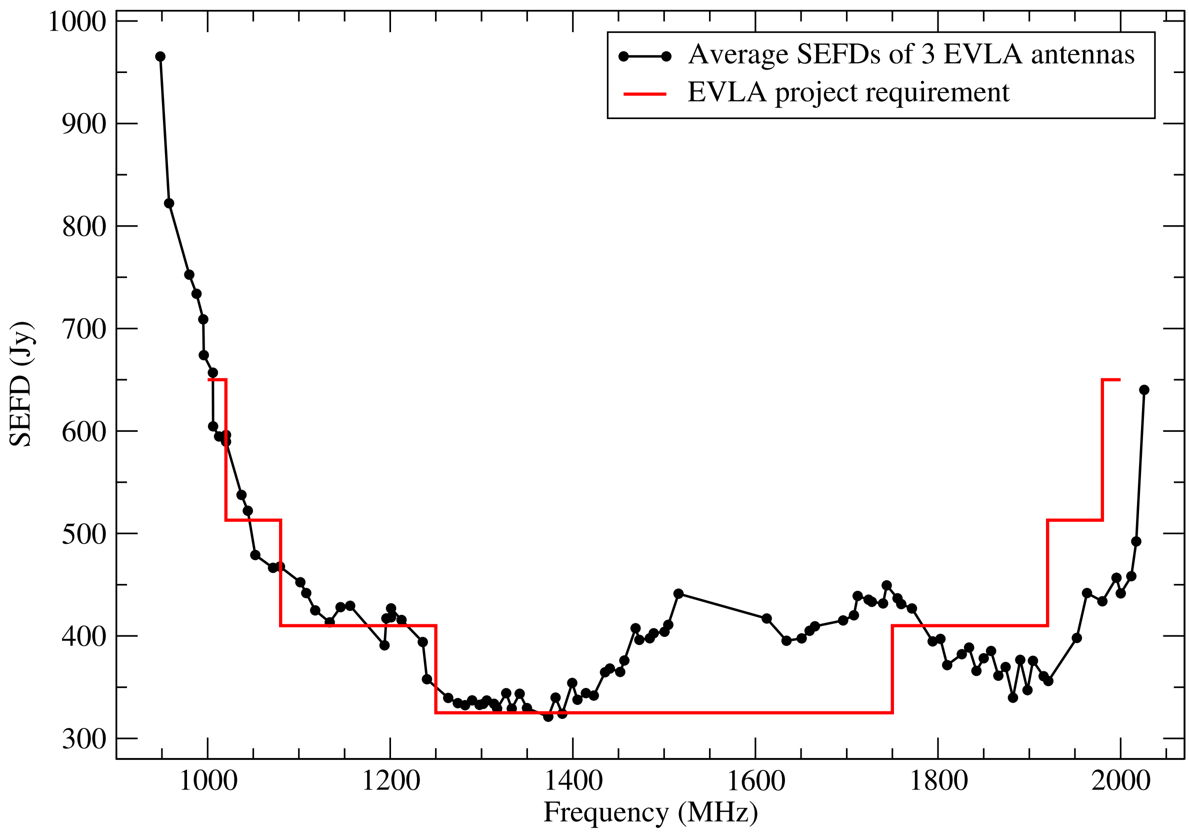

Figure 2: The SEFD values of the EVLA at L-band. No sensitivity measurements are available in the frequency range 1520–1610 MHz, because the data were severely affected by RFI. The red line denotes the EVLA project requirements on the antenna sensitivity at L-band.

5 Discussion

As shown in Figure 2, below 1425 MHz and above 1750 MHz, the measured SEFD values are consistent with the EVLA project requirements to well within $\sim 10\%$. However, the sensitivity in the frequency range 1425–1750 MHz is worse than the project requirement by 12 to up to 38%.

EVLA Memo #119 (Perley & Hayward, 2008) reports the sensitivity measurements of two EVLA antennas across the full L-band. One of these antennas was equipped with the prototype EVLA OMT, while the other antenna was equipped with an EVLA receiver that had the old-style VLA OMT. At the time, neither antenna had the 4th compressor. The current work is the average of three EVLA antennas with the final EVLA receiver systems, and the reported SEFDs lie about halfway between the measurements of the two antennas in Memo #119.

Similar to our results, the SEFDs of the two antennas in Memo #119 show a loss of sensitivity between $\sim$ 1425–1800 MHz when compared to the frequency range $\sim$ 1250–1425 MHz. Per Figure 6 in EVLA Memo #109 (Perley & Hayward, 2007), the loss in sensitivity between 1425 and 1800 MHz is caused by a drop in the antenna efficiency, whose origin presumably lies in the feed horn illumination pattern.